Available online at www.sciencedirect.com
SCIENCE DIRECT
Journal of Power Sources 155 (2006) 340–352
JOURNAL OF POWER SOURCES
www.elsevier.com/locate/jpowsour

Thermodynamic equilibrium calculations of hydrogen production from the combined processes of dimethyl ether steam reforming and partial oxidation

Troy A. Semelsberger*, Rodney L. Borup

Materials Science & Technology Division, Los Alamos National Laboratory, P.O. Box 1663, Mail Stop J579, Los Alamos, NM 87545, USA

Received 21 March 2005; accepted 22 April 2005
Available online 27 June 2005

Abstract

Thermodynamic analyses of producing a hydrogen-rich fuel-cell feed from the combined processes of dimethyl ether (DME) partial oxidation and steam reforming were investigated as a function of oxygen-to-carbon ratio (0.00–2.80), steam-to-carbon ratio (0.00–4.00), temperature (100 °C–600 °C), pressure (1–5 atm) and product species.

Thermodynamically, dimethyl ether processed with air and steam generates hydrogen-rich fuel-cell feeds; however, the hydrogen concentration is less than that for pure DME steam reforming. Results of the thermodynamic processing of dimethyl ether indicate the complete conversion of dimethyl ether to hydrogen, carbon monoxide and carbon dioxide for temperatures greater than 200 °C, oxygen-to-carbon ratios greater than 0.00 and steam-to-carbon ratios greater than 1.25 at atmospheric pressure ($P = 1$ atm). Increasing the operating pressure has negligible effects on the hydrogen content. Thermodynamically, dimethyl ether can produce concentrations of hydrogen and carbon monoxide of 52% and 2.2%, respectively, at a temperature of 300 °C, and oxygen-to-carbon ratio of 0.40, a pressure of 1 atm and a steam-to-carbon ratio of 1.50. The order of thermodynamically stable products (excluding H_2, CO, CO_2, DME, NH_3 and H_2O) in decreasing mole fraction is methane, ethane, isopropyl alcohol, acetone, *n*-propanol, ethylene, ethanol and methyl-ethyl ether; trace amounts of formaldehyde, formic acid and methanol are observed.

Ammonia and hydrogen cyanide are also thermodynamically favored products. Ammonia is favored at low temperatures in the range of oxygen-to-carbon ratios of 0.40–2.50 regardless of the steam-to-carbon ratio employed. The maximum ammonia content (i.e., 40%) occurs at an oxygen-to-carbon ratio of 0.40, a steam-to-carbon ratio of 1.00 and a temperature of 100 °C. Hydrogen cyanide is favored at high temperatures and low oxygen-to-carbon ratios with a maximum of 3.18% occurring at an oxygen-to-carbon ratio of 0.40 and a steam-to-carbon ratio of 0.00 in the temperature range of 400 °C–500 °C. Increasing the system pressure shifts the equilibrium toward ammonia and hydrogen cyanide.

Keywords: Fuel cells; Hydrogen; Methanol; DME; Alternative fuel; Reforming

1. Introduction

Multinational research efforts on alternative and renewable energy technologies to reduce pollutant emissions and to increase the efficiency of energy use are in progress. Oil is the primary energy source for transportation for many parts of the world; however even with the advent of more efficient methods of producing power, such as fuel cells, this dependency is only relaxed. Considering that China in 2000 imported 33% of its petroleum, and China's vehicle population is estimated to increase from 16.56 million in 2000 to 65.38 million in 2010 [1], the importance of an alternative transportation fuel is apparent.

Dimethyl ether is considered a promising candidate to decrease pollutants and to decrease petroleum imports. The production of dimethyl ether occurs over zeolite-based catalysts with synthesis gas as the raw material [2–13]. With

* Corresponding author. Tel.: +1 505 665 4766; fax: +1 505 665 9507.
E-mail address: troy@lanl.gov (T.A. Semelsberger).

0378-7753/$ – see front matter © 2005 Elsevier B.V. All rights reserved.
doi:10.1016/j.jpowsour.2005.04.031

synthesis gas as the raw material, dimethyl ether can be produced by any carbon containing compounds—coal and methane being the primary sources of syngas. New and more economical routes of producing dimethyl ether are being researched [3,5,6,8,14].

Most of the research with dimethyl ether in the literature relates to its oxidation [15–24] with anticipated uses as a diesel substitute [1,25–36], a household heating fuel [5,37–40] and a household cooking fuel [5,37–41]. As a diesel substitute, dimethyl ether (cetane #: 55–60) decreases NO_x, SO_x and particulate matter emissions [17,27,35,42–45]. Additional research includes direct dimethyl ether fuel cells.

Currently, there are no known studies that have been published involving the autothermal reforming of dimethyl ether. There are, however, studies detailing the steam reforming aspects of dimethyl ether [46–53] to produce hydrogen. Dimethyl ether steam reforming has been experimentally observed to proceed at temperatures comparable to methanol steam reforming (i.e., 250 °C–300 °C) [47,52,53], with a hydrogen production rate of 92 mmoles g_{cat}^{-1} h^{-1} (at $T = 275$ °C, S/C = 1.50, $\tau = 1.00$ s and $P_{amb} = 0.78$ atm) [49,50,54].

The general approach to dimethyl ether steam reforming has been to acid catalyze DME to methanol followed by methanol steam reforming to produce hydrogen. The solid acid catalyst typically employed for the hydrolysis of dimethyl ether to methanol is γ-Al_2O_3 (additional solid acid catalysts include zeolites [49,50,52,54] and HPA [47]). Recent studies [54,55] report the effects of various acid catalysts (zeolites, zirconia, silica, γ-Al_2O_3, etc.) on the hydrolysis of dimethyl ether to methanol. The results indicate that γ-Al_2O_3 and zeolites produce methanol concentrations that approach those predicted by thermodynamics [48]. The catalytic components (typically Cu/Zn) for methanol steam reforming have been well documented elsewhere.

1.1. Scope

This paper presents the thermodynamics of producing hydrogen-rich fuel-cell feeds from the combined processes of dimethyl ether partial oxidation and steam reforming. This study explores the equilibrium compositions as a function of steam-to-carbon ratio (0.00–4.00), oxygen-to-carbon ratio (0.00–2.80), pressure (1–5 atm) and temperature (100 °C–600 °C). The product set, or species considered were hydrogen, carbon monoxide, carbon dioxide, acetylene, ethanol, methanol, ethylene, methyl-ethyl ether, formaldehyde, formic acid, acetone, *n*-propanol, ethane, ammonia, hydrogen cyanide and isopropyl alcohol. Details of the calculations and the tabulated results for both dimethyl ether steam reforming and dimethyl ether partial oxidation can be found in LA-14187 at http://www.osti.gov/bridge/. This report is available upon request.

2. Hydrogen producing processes

This section addresses the implications of producing hydrogen-rich fuel-cell feeds from the processes of partial oxidation and/or steam reforming using an on-board automotive fuel processor. For illustration, the continuum of operating conditions available for producing hydrogen is depicted in Fig. 1. The salient features of operating a fuel processor are hydrogen production, carbon monoxide production, overall efficiency and startup energy.

The highest hydrogen reforming efficiency occurs at the highest hydrogen content. The production of carbon monoxide is an inefficient by-product that impacts the overall size and mass of the fuel processor—specifically the high and low temperature water-gas shift reactors. Increasing the size and mass of the fuel processor leads to an increased amount of energy needed to raise the fuel processor from ambient conditions to the desired operating temperature defined as the start-up energy. Automotive fuel processors also require frequent start-ups and shutdowns, thus implying both transient and "steady-state" operations.

Optimizing an automotive fuel processor necessitates optimizing it at numerous operating conditions (transient, steady-state, idling, accelerating, etc.) and taking into account system integration. Because of the complexities of optimizing a fuel-cell-powered fuel-processor-based automotive system, the processes of steam reforming and partial oxidation for generating hydrogen-rich fuel-cell feeds will be broadly described.

The maximum hydrogen production efficiency (η_{H_2}) occurs under steam reforming conditions (right-hand side of

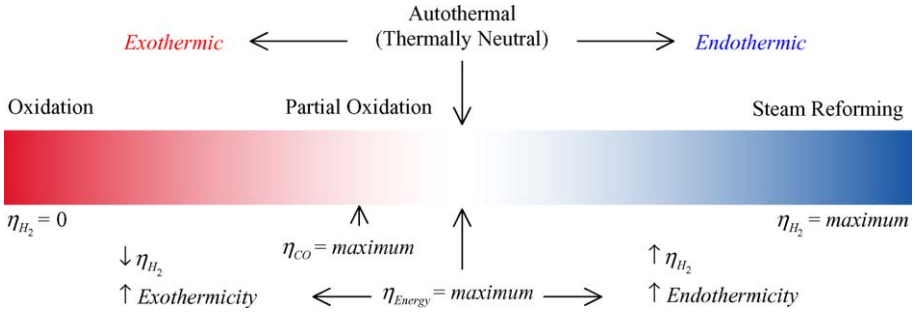

Fig. 1. Continuum of operating conditions for producing hydrogen-rich fuel-cell feeds from partial oxidation and steam reforming processes.

Fig. 1), while the minimum hydrogen production efficiency of zero occurs for the process of complete oxidation (left-hand side of Fig. 1). As the operation moves from pure steam reforming to oxidation (right to left in Fig. 1) the hydrogen production efficiency decreases while the carbon monoxide content increases, reaching a maximum when operating under partial oxidation conditions. The global minimum of carbon monoxide occurs under complete oxidation—this process is not realistic when hydrogen is the desired product. Complete oxidation could be employed for rapid heating if the only product sought is heat energy. The local minimum of carbon monoxide, considering that hydrogen is to be produced, occurs at the conditions of pure steam reforming.

From the standpoint of energy efficiency, the maximum occurs while operating under autothermal conditions (Fig. 1)—a combination of steam reforming (endothermic) and partial oxidation (typically exothermic) processes [56]. Operating autothermally, the partial oxidation reaction supplies the energy required to drive the steam reforming reaction. Autothermal is the condition when the net enthalpy is identically zero (i.e., thermally neutral), but this term has been used in general to describe the combined processes of partial oxidation and steam reforming. In this paper, autothermal operation is defined as the condition of thermal neutrality. The maximum endotherm occurs under steam reforming conditions, while the maximum exotherm occurs under complete oxidation.

What are the optimal processing conditions that will produce a maximum hydrogen production efficiency, the least amount of carbon monoxide and the highest overall energy efficiency? This nontrivial answer lies in the region between partial oxidation and steam reforming—assuming the process is operating under steady-state conditions where rapid heating is not required. The combination of partial oxidation and steam reforming will be determined by the system under consideration. If a small amount of heat is required, then the process will be operated slightly exothermic, at the cost of producing more carbon monoxide and less hydrogen. If the process is operated slightly endothermic, then the system requires an external heat source (i.e., a burner or interstage heaters). In the absence of waste heat streams (i.e., heat generated within the fuel cell) or the need to generate a heat stream (i.e., for fuel vaporization), the optimal processing occurs under autothermal conditions.

3. Modeling methodology

3.1. Gibb's free energy

Equilibrium compositions were calculated by the minimization of the Gibb's free energy. The Gibb's free energy equations that were minimized are shown in Eq. (1). A derivation of these equations is given in Perry's Chemical Engineers' Handbook [57].

$$\Delta G_{fi}^{o} + RT\ln P + RT\ln y_i + RT\ln\hat{\phi}_i + \sum_k(\lambda_k a_{ik}) = 0, \tag{1}$$

Subject to the constraints,

$$\sum_i(y_i a_{ik}) = \frac{A_k}{\sum_i n_i} \quad \text{and} \quad \sum_i y_i = 1,$$

where $\Delta G_{f,i}^{\circ}$ is the standard Gibb's function of formation of compound i, R the molar gas constant, T the processing temperature, P the processing pressure, y_i the gas phase mole fraction of compound i, $\hat{\phi}_i$ the fugacity coefficient of compound i, λ_k the Lagrange multiplier, $a_{i,k}$ the number of atoms for the kth element of species i, A_k the total mass of the kth element and n_i is the moles of compound i.

All equilibrium calculations were performed with vapor phase constituents. The equation of state used was the Peng–Robinson equation. Minimization was accomplished with the use of Aspen Tech™, commercial software capable of performing multicomponent equilibria.

The modeling methodology is represented by the flow chart in Fig. 2. The four "steps" to calculating chemical equilibrium are:

1. choose reactants and their relative proportions;
2. choose products;
3. choose processing temperature and pressure;
4. perform minimization.

3.2. DME processing: primary reactions, temperatures and pressures

The primary reactions and temperatures (100 °C–600 °C) chosen for the initial equilibrium modeling were based on the combined processes of dimethyl ether partial oxidation and steam reforming. The reactions, or equivalently, the constrained equilibria, for both the endothermic and exothermic processes are as follows:

Exothermic reactions

DME partial oxidation:

$$CH_3OCH_3 + 0.5O_2 \rightleftharpoons 2CO + 3H_2$$

$$\Delta H_{rxn}^{o} = -25\,\text{kJ mol}^{-1}$$

DME oxidation:

$$CH_3OCH_3 + 3O_2 \rightleftharpoons 2CO_2 + 3H_2O(v)$$

$$\Delta H_{rxn}^{o} = -1316\,\text{kJ mol}^{-1}$$

Endothermic reactions

DME steam reforming:

$$CH_3OCH_3 + 3H_2O(v) \rightleftharpoons 2CO_2 + 6H_2$$

$$\Delta H_{rxn}^{o} = +135\,\text{kJ mol}^{-1}$$

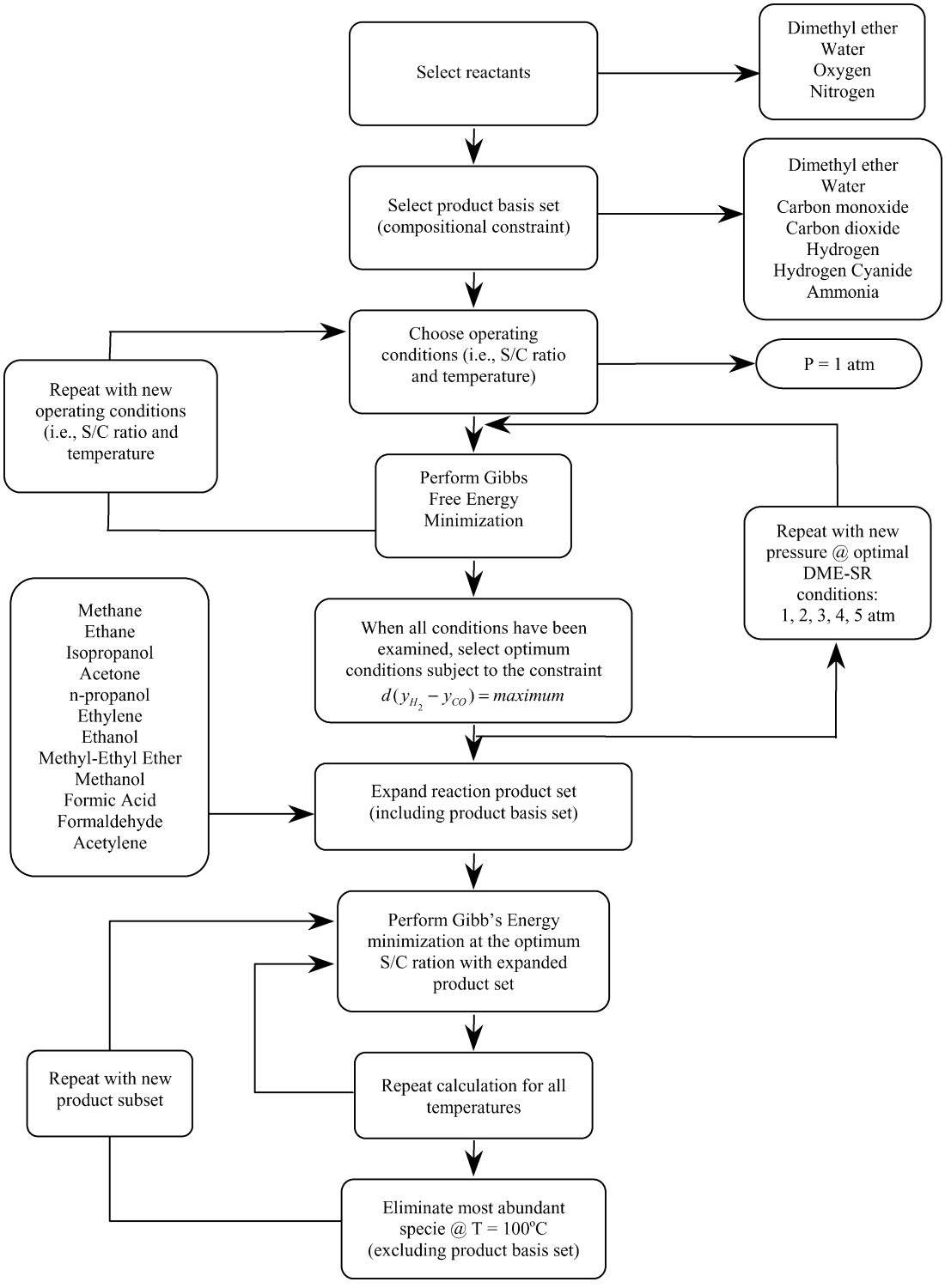

Fig. 2. Dimethyl ether steam reforming and partial oxidation modeling methodology flow chart.

Water-gas shift

$$H_2 + CO_2 \rightleftharpoons H_2O(v) + CO$$

$$\Delta H^{o}_{rxn} = +41\ \text{kJ mol}^{-1}$$

The reactants and products of the exothermic and endothermic reactions were included in the product basis set (viz, CH_3OCH_3, H_2O, CO_2, CO, H_2, N_2, O_2, NH_3 and HCN). Oxygen was fed in the form of air; therefore, nitrogen was included as a product and reactant. Two nitrogen containing compounds, ammonia (NH_3) and hydrogen

cyanide (HCN), were also included in the product basis set.

Ammonia and hydrogen cyanide were included to determine the appropriate conditions for their generation. While ammonia is a poison to PEM fuel cells, other applications favor ammonia formation; on-board generation of ammonia can be used to reduce NO_x emissions from lean-burn engines [58–64]. Hydrogen cyanide is a poison to both PEM fuel cells and people; it is immediately fatal at a concentration of 496 ppb and lethal at an exposure time of 30 min at 248 ppb. Although hydrogen cyanide has not been observed in industrial practice during partial oxidation or the complete oxidation of hydrocarbon fuels, it was included as a product due to its high toxicity. Ammonia and hydrogen cyanide were calculated to have low equilibrium concentrations thus are minor species; the low equilibrium concentrations predicted for NH_3 and HCN do not significantly alter the concentrations of the major species.

The thermodynamic modeling of the combined processes of dimethyl ether partial oxidation and steam reforming with the product basis set consisted of varying the oxygen-to-carbon ratio, steam-to-carbon ratio, temperature and pressure. Oxygen-to-carbon ratios studied ranged from 0.00 to 2.80, steam-to-carbon ratios from 0.00 to 4.00 and temperatures and pressures from 100 °C to 600 °C and 1–5 atm.

Given the processing temperatures and products, the equilibrium compositions were calculated. The equilibrium compositions were mapped for each condition, and an optimal processing temperature and feed composition were determined. The processing pressure was then varied to ascertain its effects on the equilibrium composition.

3.3. DME-SR: thermodynamically feasible products

Depending on the operating conditions (specifically the catalysts employed), the product distribution may be different than those assumed above. The product set was expanded to include products that may be intermediates or products from side reactions. The expanded product set is shown in Table 1.

Table 1
Expanded product set used for the determination of thermodynamically feasible products for the combined processes of dimethyl ether steam reforming and partial oxidation

Expanded product set	
Acetone	Hydrogen[a]
Acetylene	Hydrogen cyanide[a]
Ammonia[a]	Isopropanol
Carbon dioxide[a]	Methane
Carbon monoxide[a]	Methanol
Dimethyl ether (DME)[a]	Methyl-ethyl ether
Ethane	Nitrogen[a]
Ethanol	Oxygen[a]
Ethylene	*n*-Propanol
Formaldehyde	Water[a]
Formic acid	

[a] Product basis set.

To further explore the thermodynamically feasible products under various degrees of selectivity, the species with the largest effluent mole fraction was removed from the product set with the exception of the products in the basis set; then, the calculations were repeated, thus defining a new thermodynamic case study. In all cases, the product sets excluded carbon as a thermodynamically viable species.

4. Results

Because a primary goal of fuel reforming for fuel cells is to produce the largest amount of hydrogen while concertedly producing the least amount of carbon monoxide, the thermodynamic results are presented in the context of hydrogen and carbon monoxide. Selected plots were chosen to give the general sensitivity of the process variables (i.e., temperature, pressure, oxygen-to-carbon ratio and steam–carbon ratio) on the production of hydrogen and carbon monoxide and are shown on a wet nitrogen basis.

4.1. DME SR-POx: hydrogen effluent mole fraction

4.1.1. Constant steam-to-carbon ratios

The production of hydrogen as a function of temperature and oxygen-to-carbon ratio for steam-to-carbon ratios of 0.25, 0.50, 1.50 and 4.00 and a pressure of 1 atm are depicted in Fig. 3. The conditions that produce the largest effluent mole fractions of hydrogen occur under pure steam reforming conditions (O/C = 0.0), with the global maximum of hydrogen at 72% occurring at a steam-to-carbon ratio of 1.50, a pressure of 1 atm and a temperature of approximately 300 °C (Fig. 3c). Operating under pure steam reforming conditions, the production of hydrogen is non-monotonic with respect to temperature at a given steam-to-carbon ratio and is also nonmonotonic with respect to steam-to-carbon ratio at a given temperature.

The hydrogen content is a strong function of oxygen-to-carbon ratio; the hydrogen content at a steam-to-carbon ratio of 1.50 and a temperature of 300 °C decreases from 52% to 38% when the oxygen-to-carbon ratio is increased from 0.40 to 0.80. The strong functional dependence of the hydrogen content on oxygen-to-carbon ratio is a direct consequence of fuel oxidation and nitrogen dilution. Increasing the oxygen-to-carbon ratio beyond 0.50 introduces more oxygen than required for partial oxidation, thus a transitioning from partial oxidation to complete oxidation takes place above 0.50.

The hydrogen content is a weak function of temperature for temperatures greater than 200 °C; for a steam-to-carbon ratio of 1.50 and an oxygen-to-carbon ratio of 0.40, the hydrogen content decreases from 52% to 45% when the temperature is increased from 300 °C to 600 °C. The decrease in hydrogen content is primarily due to the water-gas shift reaction equilibrium. The amount of hydrogen produced in the combined processes of dimethyl ether steam reforming

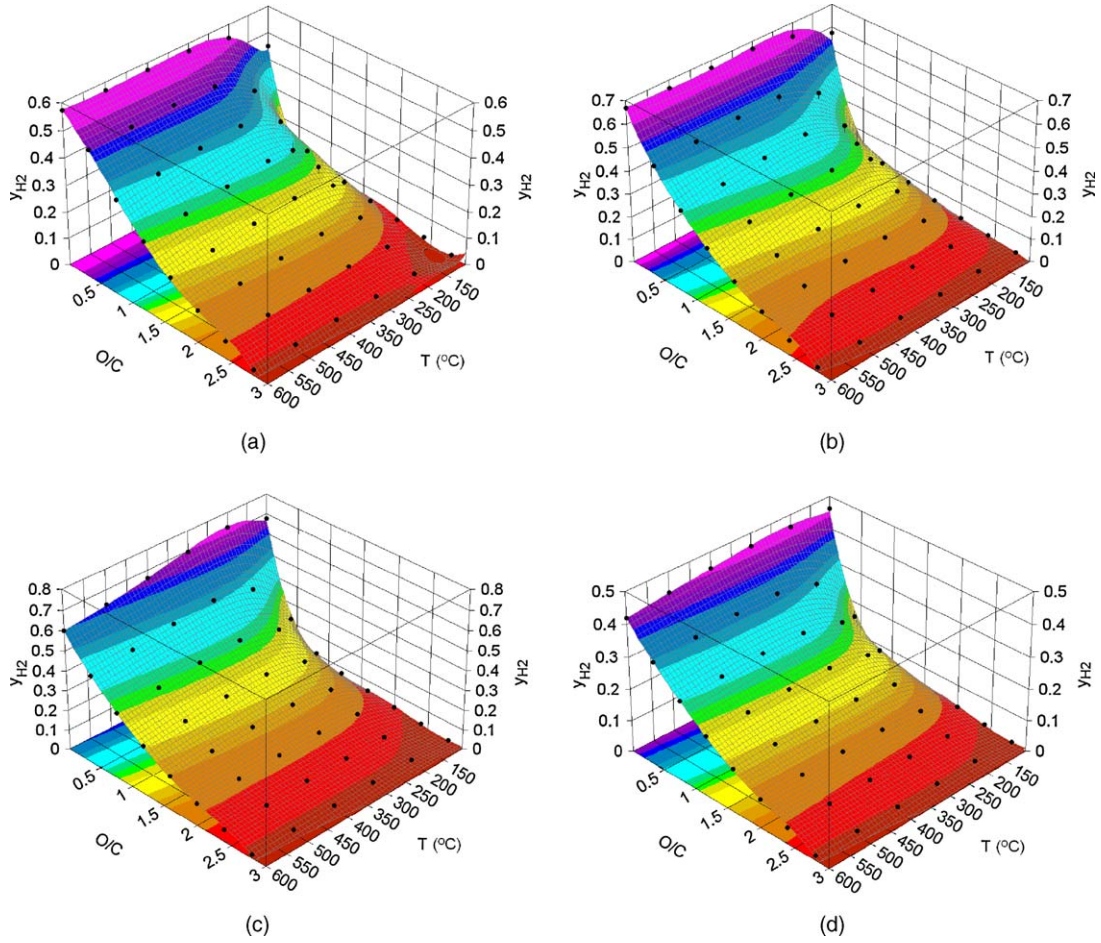

Fig. 3. Plot of the thermodynamic equilibrium product mole fractions of hydrogen on a wet-nitrogen basis given a steam-to-carbon ratio of (a) 0.25, (b) 0.50, (c) 1.50 and (d) 4.00 as a function of oxygen-to-carbon ratio and temperature for the combined processes of dimethyl ether steam reforming and partial oxidation: $P = 1$ atm.

and partial oxidation will be less than the amount produced through dimethyl ether steam reforming.

4.1.2. Constant oxygen-to-carbon ratios

An alternate way of displaying the production of hydrogen is to plot it as a function of temperature and steam-to-carbon ratio for given oxygen-to-carbon ratios (Fig. 4a–d). The data presented are for oxygen-to-carbon ratios of 0.40, 0.80, 2.00 and 2.80.

The effluent mole fractions of hydrogen as a function of steam-to-carbon ratio and temperature exhibit maxima given constant oxygen-to-carbon ratios. Hydrogen maxima occur at a temperature of 300 °C for steam-to-carbon ratios less than or equal to 1.50. The decrease in the hydrogen mole fraction as the steam-to-carbon ratio is increased is due to steam dilution. Although increasing the amount of steam shifts the water-gas-shift equilibrium to the left toward hydrogen and carbon dioxide, the shift in equilibrium is small compared to the effects of steam dilution. If the effects of steam dilution are removed, then the hydrogen content increases according to the water-gas-shift equilibrium.

The maximum amount of hydrogen that can be generated occurs at an oxygen-to-carbon ratio of 0.0, and monotonically decreases as the oxygen-to-carbon ratio increases (Figs. 3 and 4). The addition of oxygen decreases the hydrogen content illustrated by the decrease in the hydrogen effluent mole fraction maxima at 300 °C from 51% to 45% to 14% to 2% as the oxygen-to-carbon ratio is increased from 0.40 to 0.80 to 2.00 to 2.80. This is due to the increased fraction of dimethyl ether fully oxidized and because of nitrogen dilution.

4.2. DME SR-POx: carbon monoxide effluent mole fraction

4.2.1. Constant steam-to-carbon ratios

The carbon monoxide effluent mole fractions as a function of temperature and oxygen-to-carbon ratio for steam-to-carbon ratios of 0.25, 0.50, 1.50 and 4.00 are depicted in Fig. 5a–d. Carbon monoxide is generated through three processes: the water-gas shift reaction, "partial steam reforming" and partial oxidation. At a given steam-to-carbon ratio,

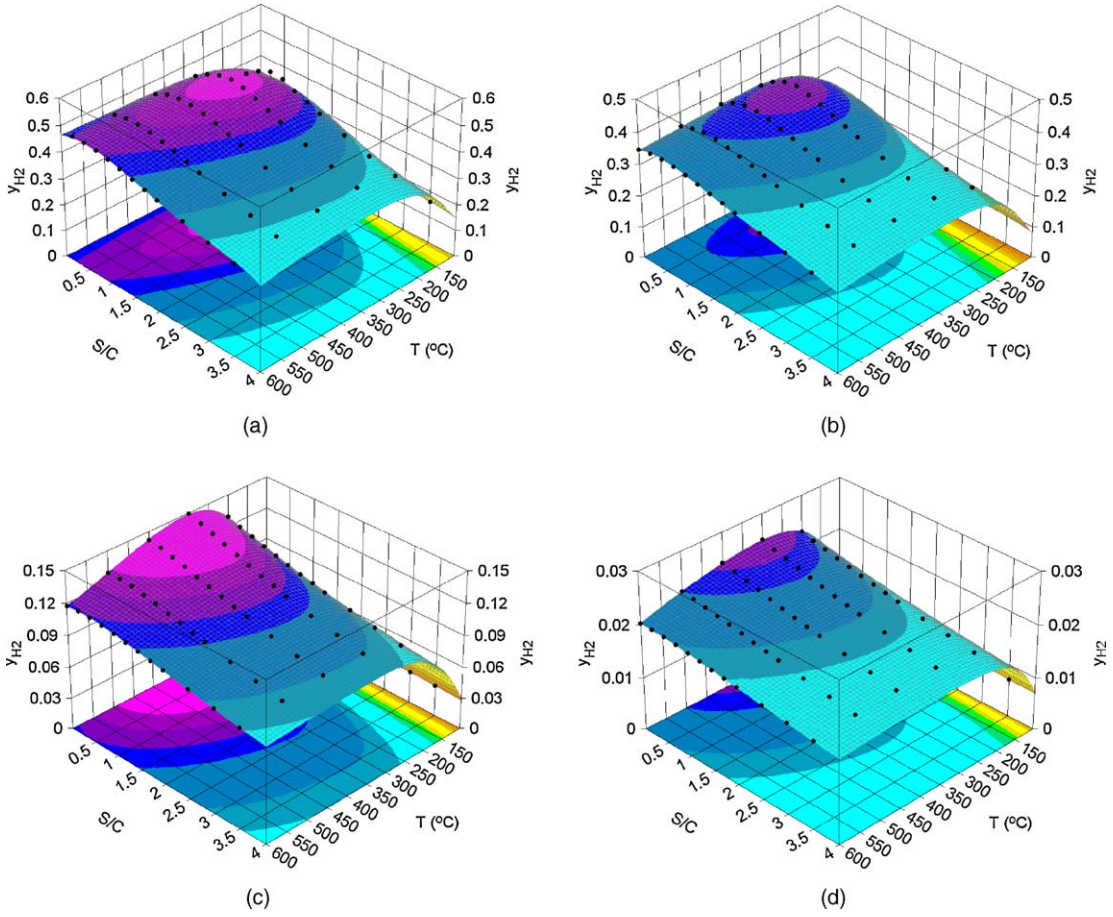

Fig. 4. Plot of the thermodynamic equilibrium product mole fractions of hydrogen on a wet-nitrogen basis given an oxygen-to-carbon ratio of (a) 0.40, (b) 0.80, (c) 2.00 and (d) 2.80 as a function of steam-to-carbon ratio and temperature for the combined processes of dimethyl ether steam reforming and partial oxidation.

the amount of carbon monoxide decreases with increasing oxygen-to-carbon ratio because of the increased fraction of dimethyl ether that is fully oxidized and increases with increasing temperature due to the water-gas shift equilibrium. The maximum carbon monoxide content is 33%, and occurs at a steam-to-carbon ratio of 0.50, oxygen-to-carbon ratio of 0.00 and a temperature of 600 °C. At these conditions, the overall reaction which generates carbon monoxide is "partial steam reforming":

$$CH_3OCH_3 + H_2O(v) \rightleftharpoons 4H_2 + 2CO$$

$$\Delta H^{o}_{rxn} = +217\,kJ\,mol^{-1}.$$

Under partial oxidation conditions with an oxygen-to-carbon ratio of 0.40 and a steam-to-carbon ratio of 0.00, the maximum carbon monoxide content is 29% at 300 °C; on a nitrogen-free basis the carbon monoxide content is 37%. Nitrogen dilution effects are also observed with hydrogen.

Increasing the steam-to-carbon ratio from 0.50 to 4.00 shifts the equilibrium towards carbon dioxide and hydrogen via the water-gas-shift reaction, thus decreasing the amount of carbon monoxide. Increasing the amount of water also increases the effects of steam dilution where the carbon monoxide content decreases faster because of the addition water than with the shift of the water-gas shift equilibrium.

4.2.2. Constant oxygen-to-carbon ratios

Carbon monoxide concentrations plotted as a function of steam-to-carbon ratio and temperature, given oxygen-to-carbon ratios of 0.40, 0.80, 2.00 and 2.80, are presented in Fig. 6a–d. Increasing the oxygen-to-carbon ratio from 0.40 to 2.80 at a steam-to-carbon ratio of 1.50 and a temperature of 300 °C decreases the amount of carbon monoxide from 2.20% to 0.02%, primarily because of complete oxidation of dimethyl ether and nitrogen dilution. The carbon monoxide effluent mole fraction maxima occur at high temperatures (e.g., 600 °C) and low steam-to-carbon ratios (e.g., 0.00).

Comparing Figs. 5 and 6 illustrates the sensitivity of dilution (both nitrogen and steam), oxygen-to-carbon ratio and steam-to-carbon ratio on the carbon monoxide effluent mole fractions. For the case of constant steam-to-carbon ratio (Fig. 5), the decrease in carbon monoxide content can be attributed to steam dilution; however, for the case of constant oxygen-to-carbon ratio (Fig. 6), the decrease can be attributed to the oxidation of dimethyl ether as the oxygen-to-carbon ratio increases.

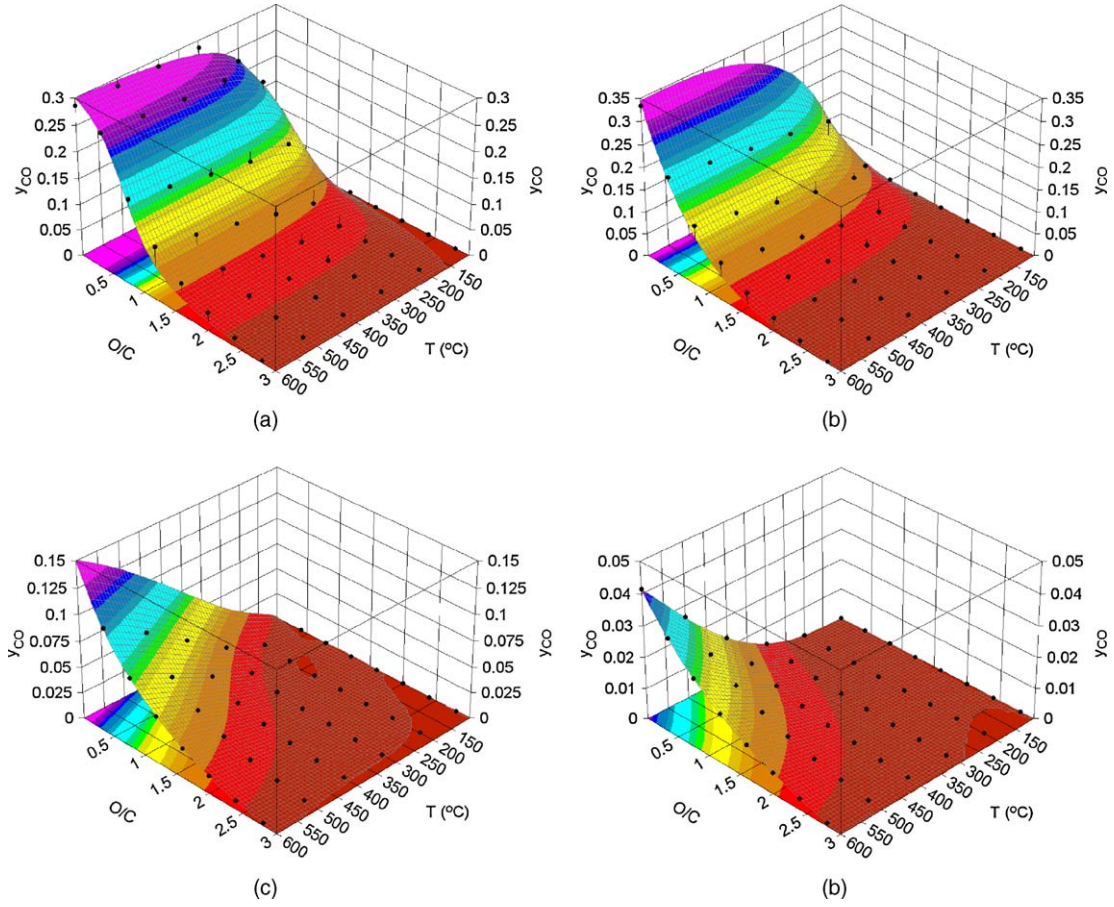

Fig. 5. Plot of the thermodynamic equilibrium product mole fractions of carbon monoxide on a wet-nitrogen basis given a steam-to-carbon ratio of (a) 0.25, (b) 0.50, (c) 1.50 and (d) 4.00 as a function of oxygen-to-carbon ratio and temperature for the combined processes of dimethyl ether steam reforming and partial oxidation.

4.3. DME SR-POx: ammonia effluent mole fraction

Ammonia was included in the product basis set because of its impact on PEM fuel cell durability as a potential hydrogen impurity. The equilibrium effluent mole fraction of ammonia as a function of oxygen-to-carbon ratio and temperature at a pressure of 1 atm and steam-to-carbon ratio of 1.50 is shown in Fig. 7.

Ammonia can be produced in the presence of hydrogen and nitrogen according to the exothermic reaction,

$$N_2 + 3H_2 \underset{\sim 200\,\text{atm}}{\overset{\text{Fe}}{\rightleftharpoons}} 2NH_3$$

$$\Delta H^{\circ}_{\text{rxn}} = -92.2\,\text{kJ mol}^{-1}.$$

The thermodynamic production of ammonia is not exclusive to the partial oxidation or steam reforming of dimethyl ether; similar thermodynamic results would be expected with the processing methanol, gasoline, ethanol, methane, etc., in the presence of air and steam.

The source of nitrogen comes from air, while the primary source of hydrogen comes from dimethyl ether partial oxidation, dimethyl ether partial steam reforming, or dimethyl ether steam reforming. Thermodynamically, ammonia is produced over a wide range of oxygen-to-carbon ratios with the maximum occurring in the range of 0.50–1.50; the temperature range is 100 °C–300 °C, with a maximum ammonia production occurring at 100 °C. The narrow region of operating temperatures implies the strong functional dependence of temperature on the synthesis of ammonia.

An increase in the amount of hydrogen shifts the equilibrium to the right towards ammonia. The addition of water decreases the upper temperature limit of ammonia synthesis from 300 °C to 250 °C. Similarly, the range of oxygen-to-carbon ratios bounding the maximum amount of ammonia decreased from 0.50–1.50 to 0.40–0.80. For a steam-to-carbon ratios higher than 1.50, additional water does not effect the equilibrium composition of ammonia nor the conditions (oxygen-to-carbon ratio and temperatures) for which the maximum amount of ammonia is generated. Increasing the steam-to-carbon ratio above 1.50 the ammonia concentration decreases, but only because of steam dilution.

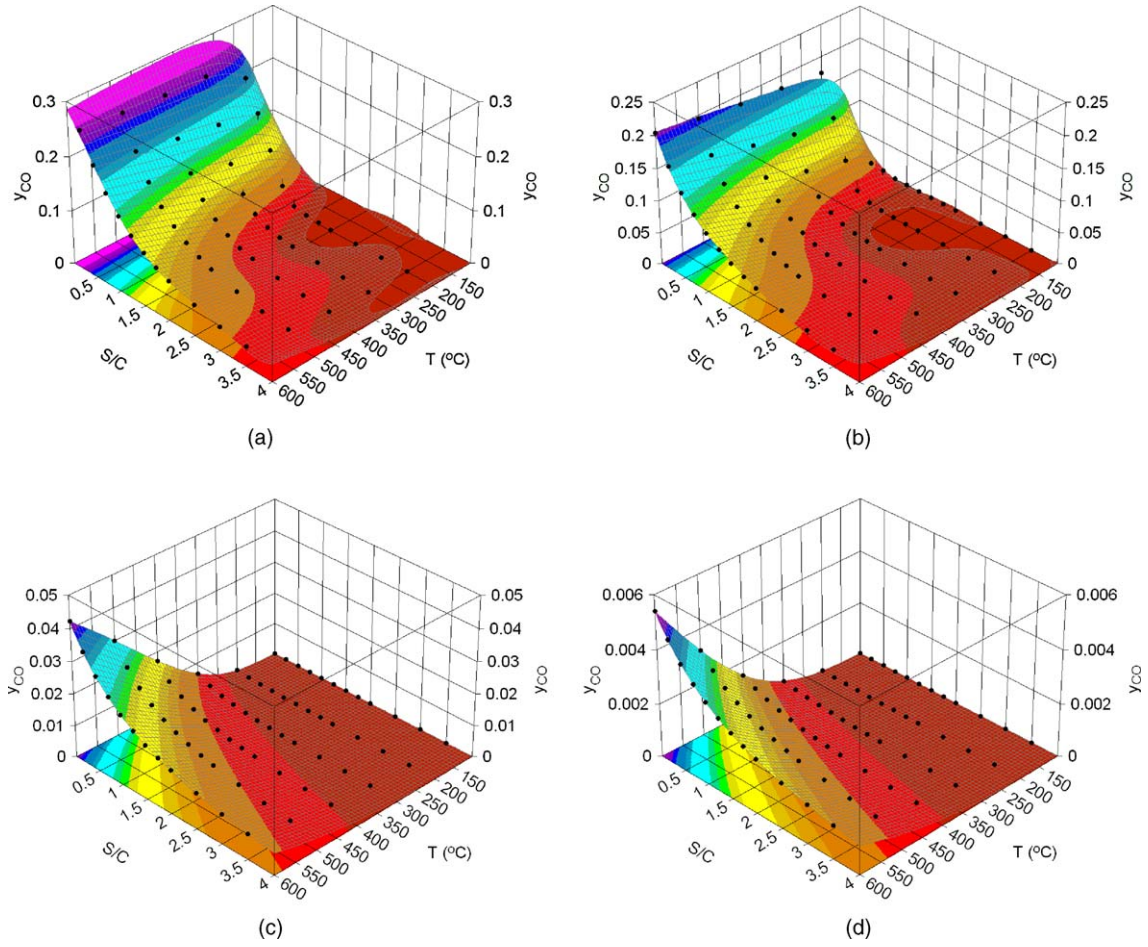

Fig. 6. Plot of the thermodynamic equilibrium product mole fractions of carbon monoxide on a wet-nitrogen basis given an oxygen-to-carbon ratio of (a) 0.40, (b) 0.80, (c) 2.00 and (d) 2.80 as a function of steam-to-carbon ratio and temperature for the combined processes of dimethyl ether steam reforming and partial oxidation.

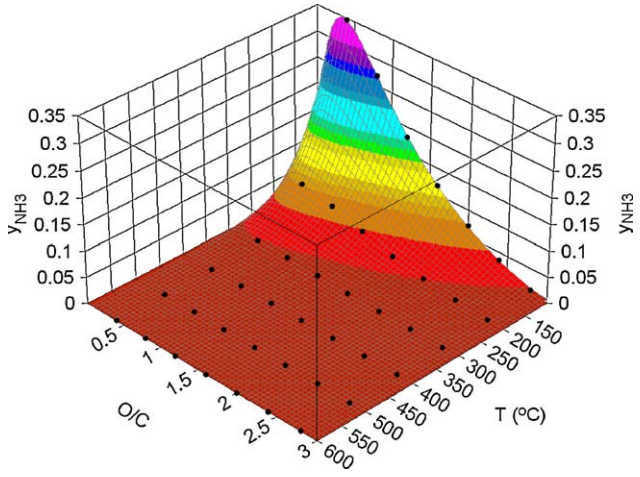

Fig. 7. Plot of the thermodynamic equilibrium product mole fractions of ammonia on a wet-nitrogen basis given a steam-to-carbon ratio of 1.50 as a function of oxygen-to-carbon ratio and temperature for the combined processes of dimethyl ether steam reforming and partial oxidation; $P = 1$ atm.

Within the constraints of the equilibrium modeling study, the effluent fractional concentrations of ammonia were negligible (i.e., in the range of ppm) for temperatures greater than 300 °C. Therefore, the concentrations of the other components in the assumed product basis set; viz., hydrogen, carbon monoxide, carbon dioxide, water and dimethyl ether, are the concentrations that would be expected if ammonia were not included in the product basis set. In contrast, for temperatures less than 300 °C, the production of ammonia does shift the equilibrium concentrations of hydrogen, carbon monoxide and carbon dioxide—this decrease does not, however, affect the thermodynamic conditions (i.e., temperature, O/C or S/C) for which hydrogen, carbon monoxide and carbon dioxide will be generated.

4.4. DME SR-POx: hydrogen cyanide effluent concentration

Analogous to ammonia, the production of hydrogen cyanide is not exclusive to the processing of dimethyl ether in the presence of air and steam. Production of hydrogen cyanide requires carbon, hydrogen and nitrogen. Carbon is

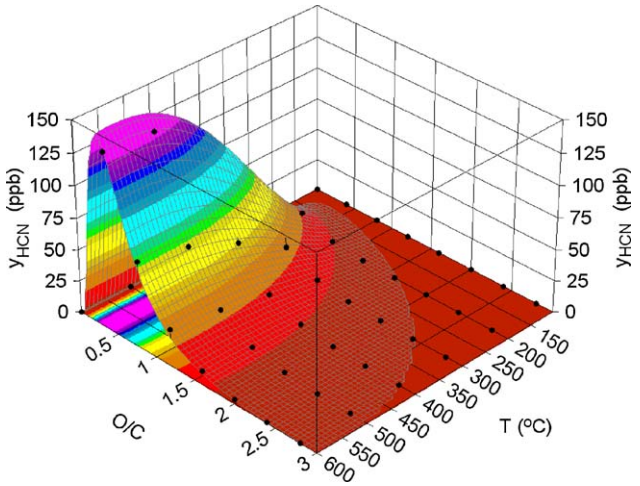

Fig. 8. Plot of the thermodynamic equilibrium product mole fractions of hydrogen cyanide on a wet-nitrogen basis at a steam-to-carbon ratio as a function of oxygen-to-carbon ratio and temperature for the combined processes of dimethyl ether steam reforming and partial oxidation.

supplied by dimethyl ether (or any other carbon containing fuel processed for hydrogen), nitrogen is supplied by air and hydrogen is generated from dimethyl ether.

The equilibrium compositions of hydrogen cyanide are presented in Fig. 8 as a function of oxygen-to-carbon ratio and temperature for a steam-to-carbon ratio of 1.50. The equilibrium compositions of hydrogen cyanide were calculated in the presence of ammonia. In the absence of steam, the hydrogen cyanide content from dimethyl ether partial oxidation was on the order of 3.0–3.5% at an oxygen-to-carbon ratio of 0.4 and a temperature of 350 °C. The addition of steam lessened the hydrogen cyanide content from percent levels to ppb levels. Hydrogen cyanide equilibrium composition of 140 ppb was calculated at a steam-to-carbon ratio of 1.50, an oxygen-to-carbon ratio of 0.40 and a temperature of 600 °C. Increasing the steam-to-carbon ratio above 1.50, the hydrogen cyanide concentration decreased by a factor because of the dilution effect. Hydrogen cyanide is most prevalent at low oxygen-to-carbon ratios and high temperatures, unlike the production of ammonia where low temperatures are required.

4.5. DME SR-POx: pressure effects

The effects of pressure on the equilibrium compositions of hydrogen, ammonia and hydrogen cyanide were investigated at a steam-to-carbon ratio of 2.00, an oxygen-to-carbon ratio of 0.40 and a temperature of 300 °C, the results are depicted in Fig. 9a–c. The pressure effects on hydrogen and carbon monoxide are negligible, as seen in Fig. 9a. The data in Fig. 9a were calculated

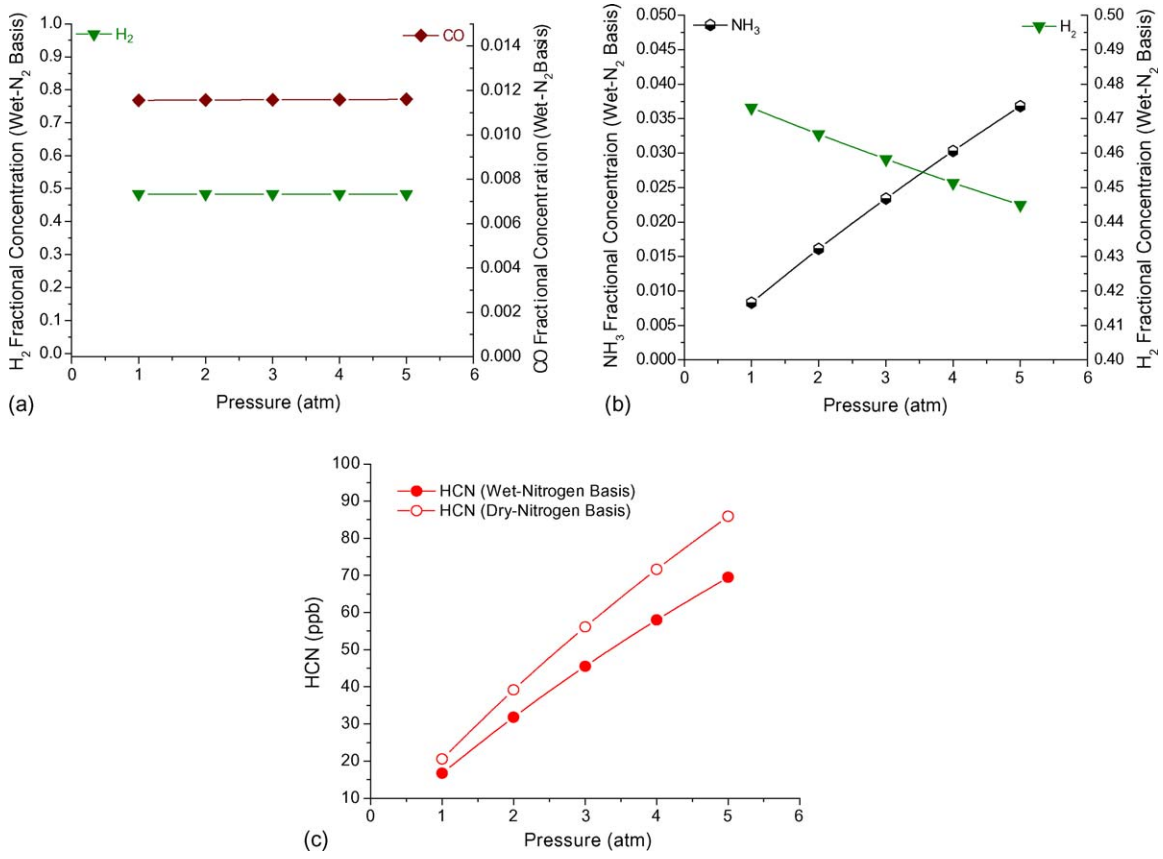

Fig. 9. Pressure effects on (a) hydrogen-excluding ammonia and hydrogen cyanide, (b) ammonia and (c) hydrogen cyanide as products at a steam-to-carbon ratio of 2.00, oxygen-to-carbon ratio of 0.40 and a temperature of 300 °C.

with the exclusion of ammonia and hydrogen cyanide as products.

Increasing the pressure from 1 to 5 atm shifts the equilibrium toward ammonia (Fig. 9b) and hydrogen cyanide (Fig. 9c). Ammonia increases from approximately 0.75% at 1 atm to approximately 37% at 5 atm, and hydrogen cyanide increases from approximately 15 ppb at 1 atm to approximately 65 ppb at 5 atm on a wet-nitrogen basis. In all cases, the conversion of dimethyl ether remained constant at 100%. The data plotted in Fig. 9b and c include the original basis set (hydrogen, carbon monoxide, carbon dioxide, ammonia, water, dimethyl ether and hydrogen cyanide).

4.6. Thermodynamically feasible products

The thermodynamic compositions of the expanded product set (Table 1) were investigated to determine other thermodynamically viable products. The species included were: acetone, acetylene, ethane, ethanol, ethylene, formaldehyde, formic acid, formic acid, isopropanol, methane, methanol, methyl-ethyl ether and *n*-propanol.

The conditions used for this investigation were a steam-to-carbon ratio of 2.00, an oxygen-to-carbon ratio of 0.40 and pressure of 1 atm; the temperature ranged from 100 °C to 600 °C. The chosen conditions do not affect the thermodynamically favored species, only the species' concentrations.

The order of the thermodynamically favored species in decreasing effluent mole fraction can be seen in Table 2. Given the manifold of product species considered, methane (thermodynamic case 1) was the most abundant, and methyl-ethyl ether (thermodynamic case 8) the least abundant. The fractional concentrations on a wet-nitrogen basis of the most abundant species as a function of temperature are shown in Fig. 10.

Methane is favored over the entire temperature range investigated, while ethane is favored in the range of 100 °C–500 °C, when methane is not considered. For thermodynamic cases 3–8, the products approach zero fractional concentration as the temperature approaches 300 °C. Methyl-ethyl ether, thermodynamic case 8, is favored but with a concentration of 1.8% at a temperature of 100 °C.

Table 2
Thermodynamic cases for expanded product set with a steam-to-carbon ratio of 2.00, an oxygen-to-carbon ratio of 0.40 and a pressure of 1 atm

Thermo case	Most abundant	Species excluded
1	Methane	None
2	Ethane	Methane
3	Isopropyl alcohol	Ethane + methane
4	Acetone	Isopropyl alcohol + ethane + methane
5	*n*-Propanol	Acetone + isopropyl alcohol + ethane + methane
6	Ethylene	*n*-Propanol + acetone + isopropyl alcohol + ethane + methane
7	Ethanol	Ethylene + *n*-propanol + acetone + isopropyl alcohol + ethane + methane
8	Methyl-ethyl ether	Ethanol + ethylene + *n*-propanol + acetone + isopropyl alcohol + ethane + methane

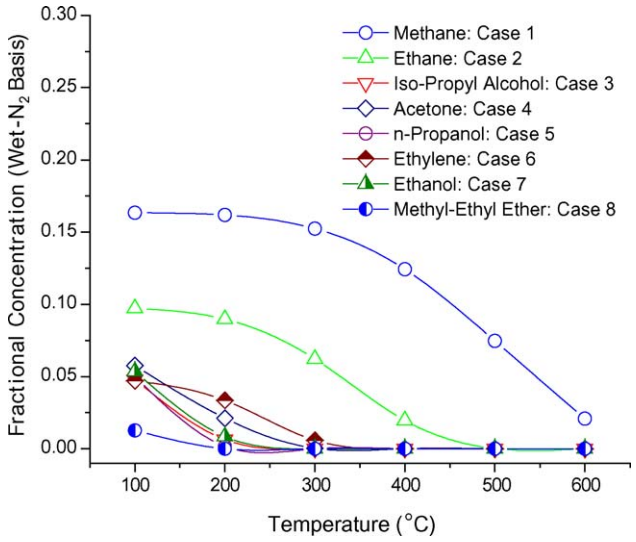

Fig. 10. Compositions (wet-nitrogen basis) of the most abundant species for thermodynamic cases 1–8 as a function of temperature at a steam-to-carbon ratio of 2.00, an oxygen-to-carbon ratio of 0.40 and a pressure of 1 atm.

Trace amounts of methanol, formaldehyde and formic acid were observed and are depicted in Fig. 11. The absence of significant amounts of these products is a direct consequence of the product basis set (specifically hydrogen, carbon dioxide and carbon monoxide). Acetylene was not observed to be favored thermodynamically. The species in the expanded product set are thermodynamically viable at defined operating conditions as shown in Fig. 10; however, they may or may not be observed experimentally depending on the catalysts employed.

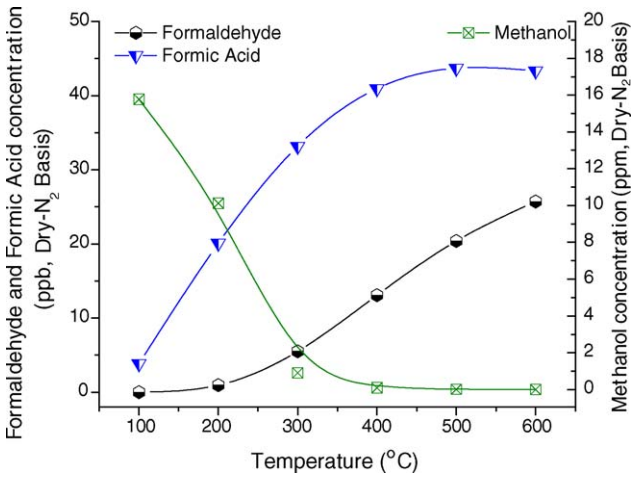

Fig. 11. Trace levels of formaldehyde, formic acid and methanol on a wet-nitrogen basis for the combined processes of dimethyl ether steam reforming and partial oxidation at a steam-to-carbon ratio of 2.00, an oxygen-to-carbon ratio of 0.40 and a pressure of 1 atm.

5. Conclusions

This study focused on the thermodynamic aspects of generating hydrogen-rich fuel-cell feeds from the combined processes of dimethyl ether steam reforming and partial oxidation. The initial study included dimethyl ether, carbon monoxide, carbon dioxide, hydrogen, ammonia and hydrogen cyanide as products; their compositions were determined as a function of temperature (100 °C–600 °C), steam-to-carbon ratio (0.00–4.00), oxygen-to-carbon ratio (0.00–2.80) and pressure (1–5 atm).

The second portion of the study expanded the product set to include acetone, acetylene, ethane, ethanol, ethylene, formaldehyde, formic acid, formic acid, isopropanol, methane, methanol, methyl-ethyl ether and *n*-propanol. The thermodynamic compositions of the expanded product set were determined as a function of temperature (100 °C–600 °C) at a steam-to-carbon ratio of 2.00, an oxygen-to-carbon ratio of 0.40 and a pressure of 1 atm. Based on the results, the following conclusions were drawn:

- Thermodynamically, dimethyl ether processed with air and steam will generate hydrogen-rich fuel-cell feeds over a wide range of temperatures (200 °C–600 °C), steam-to-carbon ratios (0.00–4.00), oxygen-to-carbon ratios (0.00–1.00) and pressures (1–5 atm). The conversion of dimethyl ether is not thermodynamically limited for temperatures greater than 200 °C, steam-to-carbon ratios greater than 1.50 and oxygen-to-carbon ratios greater than 0.00. Pressure effects are negligible on the hydrogen composition.
- The maximum production of hydrogen occurs under steam reforming conditions (i.e., oxygen-to-carbon ratio of 0.00). Increasing the steam-to-carbon ratio beyond 1.50 decreases the effluent mole fraction of hydrogen because of steam dilution. The effects of steam dilution decrease the hydrogen mole fraction faster than the increase in hydrogen because of the shift in the water-gas-shift equilibrium.
- Inclusion of oxygen (from air) as a reactant decreases the hydrogen concentration below the concentration produced from pure steam reforming. Hydrogen production at a given steam-to-carbon ratio and oxygen-to-carbon ratio is invariant under changes in temperature (200 °C–600 °C). At a given steam-to-carbon ratio, the effluent mole fraction of hydrogen monotonically decreases with increasing oxygen-to-carbon ratio because of oxidation and nitrogen dilution. A maximum hydrogen mole fraction of 52% occurred at a steam-to-carbon ratio of 1.5, an oxygen-to-carbon ratio of 0.40 and a temperature of 300 °C.
- Ammonia and hydrogen cyanide are both thermodynamically favored species. Ammonia is favored at low temperatures for the range of oxygen-to-carbon ratios of 0.50–2.50, regardless of the steam-to-carbon ratio. Ammonia production is a strong function of temperature with concentrations approaching zero for temperatures greater than 300 °C. Hydrogen cyanide is thermodynamically favored under partial oxidation conditions (i.e., steam-to-carbon ratio of 0.00) at high temperatures and low oxygen-to-carbon ratios. The addition of steam inhibits the production of hydrogen cyanide. Increasing the system pressure increases the concentration of ammonia and hydrogen cyanide.
- If the catalysts employed are not selective toward hydrogen, carbon monoxide and carbon dioxide, then additional thermodynamically favored products may be observed. The order of thermodynamically stable products generated from the combined processes of dimethyl ether steam reforming and partial oxidation was methane, ethane, isopropyl alcohol, acetone, *n*-propanol, ethylene, ethanol and methyl-ethyl ether. Trace amounts of methanol, formaldehyde and formic acid were observed.
- Equilibrium predicts that the optimum operating conditions for the reforming of DME is within the expected ranges of temperature, steam-to-carbon ratio and oxygen-to-carbon ratio of 250 °C–500 °C, 1.00–2.50 and 0.40–0.75, respectively.

References

[1] J. Song, Z. Huang, X.Q. Qiao, W.L. Wang, Energy Convers. Manag. 45 (2004) 2223–2232.
[2] F.J. Keil, Microporous Mesoporous Mater. 29 (1999) 49–66.
[3] T. Shikada, Y. Ohno, T. Ogawa, M. Ono, M. Mizuguchi, K. Tomura, K. Fujimoto, Stud. Surf. Sci. Catal. 119 (1998) 515–520.
[4] M. Stocker, Microporous Mesoporous Mater. 29 (1999) 3–48.
[5] X.M. Zheng, J.H. Fei, Z.Y. Hou, Chin. J. Chem. 19 (2001) 67–72.
[6] J. Haggin, Chem. Eng. News 69 (1991) 20–21.
[7] H.J. Kim, H. Jung, K.Y. Lee, Korean J. Chem. Eng. 18 (2001) 838–841.
[8] X.D. Peng, A.W. Wang, B.A. Toseland, P.J.A. Tijm, Industrial, Ind. Eng. Chem. Res. 38 (1999) 4381–4388.
[9] G.X. Qi, J.H. Fei, X.M. Zheng, Z.Y. Hou, React. Kinet. Catal. Lett. 73 (2001) 245–256.
[10] W.J. Shen, K.W. Jun, H.S. Choi, K.W. Lee, Korean J. Chem. Eng. 17 (2000) 210–216.
[11] T. Shikada, Y. Ohno, T. Ogawa, M. Ono, M. Mizuguchi, K. Tomura, K. Fujimoto, Kinet. Catal. 40 (1999) 395–400.
[12] Z.L. Wang, J. Diao, J.F. Wang, Y. Jin, X.D. Peng, Chin. J. Chem. Eng. 9 (2001) 412–416.
[13] M.T. Xu, J.H. Lunsford, D.W. Goodman, A. Bhattacharyya, Appl. Catal. A-Gen. 149 (1997) 289–301.
[14] Z.L. Wang, J.F. Wang, J. Diao, Y. Jin, Chem. Eng. Technol. 24 (2001) 507–511.
[15] L. Bugyi, F. Solymosi, Surf. Sci. 385 (1997) 365–375.
[16] H.J. Curran, S.L. Fischer, F.L. Dryer, Int. J. Chem. Kinet. 32 (2000) 741–759.
[17] P. Dagaut, J. Luche, M. Cathonnet, Combust. Sci. Technol. 165 (2001) 61–84.
[18] J. Sehested, T. Mogelberg, T.J. Wallington, E.W. Kaiser, O.J. Nielsen, J. Phys. Chem. 100 (1996) 17218–17225.
[19] J. Sehested, K. Sehested, J. Platz, H. Egsgaard, O.J. Nielsen, Int. J. Chem. Kinet. 29 (1997) 627–636.
[20] F. Solymosi, J. Cserenyi, L. Ovari, J. Catal. 171 (1997) 476–484.
[21] F. Solymosi, J. Cserenyi, L. Ovari, Catal. Lett. 44 (1997) 89–93.
[22] F. Solymosi, G. Klivenyi, Surf. Sci. 409 (1998) 241–251.
[23] R. Wrobel, W. Sander, E. Kraka, D. Cremer, J. Phys. Chem. A 103 (1999) 3693–3705.

[24] S.Z. Wang, T. Ishihara, Y. Takita, Appl. Catal. A-Gen. 228 (2002) 167–176.
[25] E.M. Chapman, S.V. Bhide, A.L. Boehman, L.I. Boehman and F. Waller, Engine performance and emissions from fuel blends of dimethyl ether (DME) and diesel fuel, AICHE Spring National Meeting, New Orleans, LA, 2002.
[26] Z.L. Chen, M. Konno, S. Kajitani, JSME Int. J. Ser. B-Fluids Therm. Eng. 43 (2000) 82–88.
[27] N. Elam, The Bio-DME Project (2002).
[28] D.W. Gill, H. Ofner, DME as an automotive fuel, ninth IEA Workshop, Paris, May, 2001.
[29] J.B. Hansen, S. Mikkelsen, DME as a transportation fuel (2001).
[30] International Energy Agency. DME Newsletter 3: "Dimethyl ether as automotive fuel". 1999.
[31] International Energy Agency. DME Newsletter 4: "Dimethyl ether as automotive fuel". 2000.
[32] C.L. Saricks, D.M. Rote, F. Stodolsky, J.J. Eberhardt, Energy Air Quality Fuels 2000 (2000) 86–93.
[33] S.C. Sorenson, J. Eng. Gas Turbines Power-Trans. ASME 123 (2001) 652–658.
[34] H. Yamada, K. Suzaki, A. Tezaki, Nippon Kikai Gakkai Ronbunshu, B Hen/Trans. Jpn. Soc. Mech. Eng., Part B 69 (2003) 743–750.
[35] T.C. Zannis, D.T. Hountalas, Energy Fuels 18 (2004) 659–666.
[36] J. McCandless, DME as an automotive fuel: technical, economic and social perspectives, in: Energy Frontiers Conference, 2001.
[37] T. Fleisch, Prospects for DME as a multi-purpose fuel, in: IBC Gas to Liquids Conference, Milan, Italy, 2002.
[38] T.H. Fleisch, A. Basu, M.J. Gradassi, J.G. Masin, Stud. Surf. Sci. Catal. 107 (1997) 117–125.
[39] Y. Ohno, N. Inoue, T. Ogawa, M. Ono, T. Shikada, H. Hayashi, Slurry phase synthesis and utilization of dimethyl ether, NKK Tech. Rev. (2001).
[40] M. Sun, L. Yu, C. Sun, Y. Song, J. Sun, Gen. Rev. 20 (2003).
[41] G.R. Jones, H. Holm-Larson, D. Romani, R.A. Sills, DME for power generation fuel: supplying India's southern region, in: PetroTech Conference, New Delhi, India, 2001.
[42] M. Alam, O. Fujita, K. Ito, Proc. Inst. Mech. Eng. Part A-J. Power Energy 218 (2004) 89–95.
[43] M. Alam, O. Fujita, K. Ito, Proc. Inst. Mech. Eng., Part A: J. Power Energy 218 (2004) 89–96.
[44] H.W. Wang, L.B. Zhou, D.M. Jiang, Z.H. Huang, Proc. Inst. Mech. Eng. Part D-J. Automobile Eng. 214 (2000) 101–106.
[45] H.W. Wang, L.B. Zhou, Proc. Inst. Mech. Eng. Part D-J. Automobile Eng. 217 (2003) 819–824.
[46] Bhattacharyya, Alakananda, Basu, Arunabha, Amoco Corporation, 356492 [5,498,370] (1996).
[47] V.V. Galvita, G.L. Semin, V.D. Belyaev, T.M. Yurieva, V.A. Sobyanin, Appl. Catal. A-Gen. 216 (2001) 85–90.
[48] T.A. Semelsberger, R.L. Borup, J. Power Sources, in press.
[49] T.A. Semelsberger, R.L. Borup, Hydrogen production from the steam reforming of dimethyl ether and methanol, in: 205th Electrochemical Society Meeting, San Antonio, TX, 2004.
[50] T.A. Semelsberger, R.L. Borup, J.I. Tafoya, Steam reforming of low-temperature fuels: methanol and dimethyl ether, in: Fuel Cell Seminar, San Antonio, TX, 2004.
[51] V.A. Sobyanin, S. Cavallaro, S. Freni, Energy Fuels 14 (2000) 1139–1142.
[52] Yomada, Koji, Asazawa, Koichiro, Tanaka, Hirohisa, Daihatsu Motor Co., Ltd., 653362 [6,605,559] (2003).
[53] K. Takeishi, H. Suzuki, Appl. Catal. A: Gen. 260 (2004) 111–117.
[54] T.A. Semelsberger, R.L. Borup H.L. Greene, Role of acidity on dimethyl ether steam reforming and dimethyl ether hydrolysis, in preparation.
[55] T.A. Semelsberger, K.C. Ott, R.L. Borup, H.L. Greene, Appl. Catal. B: Environ., submitted for publication.
[56] S. Ahmed, M. Krumpelt, Int. J. Hydrogen Energy 26 (2001) 291–301.
[57] R.H. Perry, D.W. Green, J.O. Maloney, Perry's Chemical Engineers' Handbook, McGraw-Hill, New York, 1999.
[58] P. Forzatti, Catal. Today 62 (2000) 51–65.
[59] R.M. Heck, Catal. Today 53 (1999) 519–523.
[60] M. Koebel, G. Madia, M. Elsener, Catal. Today 73 (2002) 239–247.
[61] W. Muller, D. Heilig, S. Meyer, G. Porten, Combust. Sci. Technol. 153 (2000) 313–324.
[62] B. Ramachandran, R.G. Herman, S. Choi, H.G. Stenger, C.E. Lyman, J.W. Sale, Catal. Today 55 (2000) 281–290.
[63] T. Valdes-Solis, G. Marban, A.B. Fuertes, Catal. Today 69 (2001) 259–264.
[64] W.E.J. van Kooten, B. Liang, H.C. Krijnsen, O.L. Oudshoorn, H.P.A. Calis, C.M. van den Bleek, Appl. Catal. B, Environ. 21 (1999) 203–213.